

# Real-Time Modeling and Control of Electric Vehicles Charging Processes

Guido Benetti, Maurizio Delfanti, *Member, IEEE*, Tullio Facchinetti, *Member, IEEE*,  
Davide Falabretti, and Marco Merlo

## I. INTRODUCTION

**S**OCIO-ECONOMIC, environmental, technical, and political factors are driving a transition in the energy sector toward a low carbon framework. In particular, the transportation sector is experiencing a huge development to reach environmental sustainability. The European Environment Agency estimated that transport is responsible for 24% of all greenhouse gas emissions in the European Economic Area member countries, 17% by road transport [1]. To reduce the environmental impact of transportation, the European Commission adopted a roadmap [2] with the target for 2050 to cut 60% of transport emissions (20% reduction by 2030).

A high electric vehicle (EV) uptake may contribute to the reduction of CO<sub>2</sub> emissions [3]. Therefore, technological development is driving a natural evolution in the transportation sector leading to electric mobility (in the following, e-mobility). The EVs initiative (EVI), a multigovernment policy forum composed of 15 members dedicated to accelerating

the introduction and adoption of EVs worldwide, set the EVs stock targets for 2020 to 20 million in EVI countries (mainly in the U.S., China, and Japan) [4]. In Italy, although today the use of EVs is still limited (1643 units in 2012), a recent study promoted by UBS forecasted a 10% penetration of full electric and plug-in hybrid vehicles by 2025 [5]. Considering the current Italian automotive market, where there are 61 cars per 100 inhabitants [6], the potential of the phenomenon can be considered very promising. However, EV deployment introduces huge technical challenges for the electric power system operation, related to the involved energy requirements.

This paper proposes a novel approach to model and to manage the e-mobility scenario. The goal is to reduce the impact of the EVs load on the power system. The envisaged method coordinates the charging processes of EVs connected to the distribution network in order to adjust their required power, avoiding overload conditions, improving the grid operational efficiency, and increasing the overall number of charge requests (CRs) that can be satisfied. The coordination policy is based on a centralized control architecture (CCA) that receives all the information required to schedule the charging processes. In this scenario, the most suitable location for installing the CCA is the distribution system operator (DSO) control center. For this purpose, an adequate communication network is required to achieve the necessary exchange of information between the CCA and the peripheral apparatuses involved in the architecture. The architecture of the networking infrastructure is beyond the scope of this paper.

The scheduler is the software component running in the CCA: it accomplishes a smart allocation of each EVs' CR in order to find the best timing of charging operations. A power flow procedure is run to check the electrical constraints on the distribution network (voltage and current limits), considering all the allocated CRs. The power flow evaluation takes into account the prediction of the load that cannot be explicitly controlled by the CCA. Given this prediction, the control strategy achieves the reduction of the peak load, considering the CRs that are dynamically made to the system. If the imposed constraints cannot be satisfied, the CR is rejected. This procedure is applied in real-time to each CR. Its application has been studied on the model of a real distribution network located in the North of Italy, confirming the ability of strongly reducing the peak load on the distribution infrastructure and to increase the number of accepted CRs.

This paper is organized as follows. Section II discusses the scientific works related to load management, with specific

Manuscript received June 15, 2014; revised October 19, 2014; accepted November 24, 2014. Date of publication December 18, 2014; date of current version April 17, 2015.

G. Benetti and T. Facchinetti are with the Department of Electrical, Computer, and Biomedical Engineering, University of Pavia, Pavia 27100, Italy.

M. Delfanti, D. Falabretti, and M. Merlo are with the Department of Energy, Politecnico di Milano, Milan 20156, Italy (e-mail: davide.falabretti@polimi.it).

Color versions of one or more of the figures in this paper are available online.

reference to EVs. The scenario of application and its modeling (i.e., the algorithm to simulate the drivers' behavior) are depicted in Sections III and IV, respectively. The novel approach proposed to schedule the CRs is depicted in Section V and Section VI deals with the numerical analysis carried out to assess the effectiveness of the proposed solution; Section VII provides an outlook of the computational performance of the algorithm developed; finally, Section VIII draws the conclusion.

## II. RELATED WORKS

One of the most challenging goals for upcoming power systems is to make effective use of technologies and solutions for the intelligent control of distributed generation (DG), to better plan and run existing electricity grids, to enable new energy services for customers, and to improve the energy efficiency in general [7]. In this direction, a main role is played by the e-mobility. On the other hand, despite the economic and environmental advantages of EVs, their increasing utilization could cause new issues for the power system operation [8], [9].

From the DSO perspective, it is extremely important to ensure that the transport capacity of electrical networks is not exceeded. In this context, in recent years, DG has been the main cause of additional investments for the refurbishment of power systems. Investments aimed to increase the so-called grid's hosting capacity [10], [11] according to grid's technical constraints: thermal limits of transformers and lines, steady-state voltage limits, and rapid voltage changes [12]–[14].

Although the hosting capacity is usually related to active users, a key issue for DSOs is to optimize the use of existing network assets, i.e., preventing the investment needed for reinforcement, while considering the growing energy request due to passive users [15] and the foreseen spread of e-mobility. A joint evaluation looking at either hosting capacity limits or maximum increase of passive loads, this last named loading capacity, is becoming more and more important [16].

On the demand side, a key issue related to the distribution network operation is the impact on the grid of increasing end-user electricity requirements, which implies the need to quantify the operational margins [17]. Focusing on EVs management, some works were proposed in the literature to schedule the charge of EVs optimally. Most of these works propose methods based on the minimization of the energy cost [17]–[20] or on the maximization of the operator's profit [21]. These methods use day-ahead forecasting techniques of the EV load to create a schedule of the charging processes. In [22], the power flow procedure is run before the optimization process. This paper uses a heuristic approach based on a particle swarm optimization to compute the allocation of EVs. In [20], the possibility of discharging batteries to provide energy to the grid is investigated. In [17] and [20], an offline optimization is performed (using quadratic and linear programming, respectively). The offline approach allows to deal with complex system constraints, regarding both the power infrastructure and the charging processes. In this case, the computational complexity does not play a significant role, since the processing is done offline. Therefore, the task may

take a long time with no impact on the applicability of the method. However, these approaches present limitations in terms of flexibility in the management of unexpected working conditions.

References [18], [19], [23], [24], and [25] are based on online procedures. In particular, De Craemer *et al.* [18] proposed a method to perform a preliminary optimization that determines the set-point for each charging station (CS). If the set-point cannot be met, the station triggers an update of the set-point. Nevertheless, in this literature work the electricity distribution infrastructure is not modeled; so, the effects of the network on the CRs' constraints, and the benefits of the scheduling procedure on the power system, are not considered. In [19], a spatially distributed optimization scheme is proposed: the power grid is divided into zones, and the optimization procedure is run for each zone independently, leading to local optima. For this reason, this method does not address network-wide issues and constraints. Di Giorgio *et al.* [25] applied a model predictive control to optimize the energy cost. The schedule is recalculated when a new charging process is requested, using a receding horizon approach to deal with the optimization time interval. The computational burden is reduced by performing the optimization on a limited section of the power network, i.e., considering that the EVs to schedule belong to the same LV feeder. Fan [24] adopts an approach based on congestion control techniques used in internet networking protocols. Although the algorithm runs in a decentralized manner, the analysis guarantees the convergence to the optimal performance in terms of customer costs. This method, however, does not take into account technical issues and constraints related to the power network operations. Deilami *et al.* [23] produce an optimal schedule of charging processes with a time resolution of 5 min, considering the constraints on the power network, and allowing for EVs random plug-in. The use of optimization techniques presents scalability issues due to the required computation time, which rapidly increases at the increasing of the EVs number and of the power infrastructure complexity. These works thus introduce specific solutions to limit the computational complexity of the optimization. Possible solutions include the reduction of the duration, or granularity, of the time window of optimization, or the reduction of the size of the network under analysis. An upper bound on the computational time required by some relevant approaches can be inferred from the data reported in [25], where the time resolution is assessed for the considered methods. Such time resolutions span from 36 s to 15 min. In [25], the method proposed in [26] is defined to have a continuous time resolution, suggesting that the control action can be computed sufficiently quickly to cope with continuous variations of the monitored physical values. This result is achieved by leveraging a sliding mode control approach. However, this paper does not present the computational issues that arise in discrete scheduling approaches.

Finally, Benetti *et al.* [27] presented the preliminary findings of the present work, focusing on the description of the case study. This paper includes neither the system model and formulation of the scheduling policy, nor a detailed analysis of simulation results.

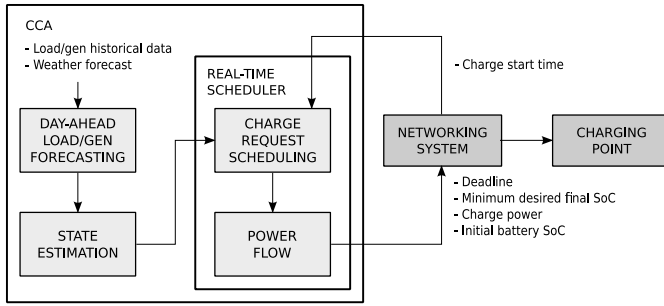


Fig. 1. System architecture supporting the CCA.

### III. SCENARIO OF APPLICATION

This section illustrates the use case considered in our approach. When the  $\lambda_i$  EV is connected to a CS at time  $r_i$ , all relevant information is collected and sent to the CCA (Fig. 1). Such information includes the following:

- 1) electric power  $P_i$  required by the CR;
- 2) initial state of charge (SoC) of the battery  $\gamma_i(r_i)$ ;
- 3) minimum desired SoC after the charge (fill level)  $\gamma_i^{th}$ ;
- 4) time  $D_i$  before which the CR must be completed (deadline).

While  $P_i$  and  $\gamma_i(r_i)$  are automatically detectable once the EV is plugged,  $\gamma_i^{th}$  and  $D_i$  are associated with user requirements. Therefore, they must be explicitly supplied to the CCA by means of a suitable human-machine interface (HMI). Due to the constraints on the peak load, some combinations of deadline and fill level may not be guaranteed. For instance, a given fill level may not be guaranteed if the deadline is too short.

Once all this information has been collected, the CCA determines the best time period when the CR should be performed. The scheduler selects the interval such that simultaneous charging processes are avoided when not strictly necessary. For instance, a CR with a long deadline can be delayed. Possible violations of electrical constraints in the selected interval are checked using a power flow procedure. To perform the check, a close cooperation with the electric grid management procedures is required. If no violation is detected, the CR is enabled, filling the battery up to the desired level  $\gamma_i^{th}$  before the imposed deadline  $r_i + D_i$ . If the CCA can not find a suitable charging interval, the CR is rejected, since it would produce an overload condition in the power system. The HMI can be implemented to alert the customer about the impossibility to complete the desired operation within the specified deadline. In this case, the user may decide to relax either the constraint on the deadline or the final fill level. The investigation on more advanced overload condition management approaches is left as future work.

If the EV leaves the CS before the time  $r_i + D_i$ , the desired SoC cannot be guaranteed. In this paper, such a case is not explicitly considered in simulating the users behavior. However, in real-life scenarios, this event can be easily detected by the CCA and the availability of spare energy can be accounted in the schedule of upcoming EVs.

### IV. SYSTEM MODEL

In order to assess the performance of the proposed CCA, suitable models have been developed for both the electric distribution grid and the EV traffic.

#### A. Electric Grid Model

The distribution network is modeled by its nodal admittance matrix, which is built on the basis of the topology and the electrical parameters of all electrical branches. The grid operational conditions change with time according to load and generation variations and power requirements of EVs in charge. All the loads and generators are considered in the power flow as active and reactive power withdrawals/injections (P, Q buses in the power-flow problem). The CSs are modeled as power absorptions in a given MV bus. It is worth noting that the LV grid is not modeled in this paper, since only public CSs are considered. According to their power requirements, typically larger than 100 kW for the assumptions adopted, they are usually connected directly to the MV grid by a dedicated MV/LV transformer or, alternatively, through a dedicated LV line sized according to the maximum power requirements of the CS [28]. In both cases, the grid infrastructure downstream the point of connection to the MV grid does not limit the number of EVs that can be simultaneously charged, thus their technical limits do not require to be considered in the scheduling process. At each time step  $t$ , a power-flow procedure based on the Newton-Raphson method is applied to assess voltages (magnitude and phase: primary unknowns) on all network buses. Afterwards, branch currents (secondary unknowns) are calculated. For each of the  $N$  buses of the network, the power-flow problem is modeled as follows:

$$\begin{cases} P_n(t) = V_n(t) \cdot \sum_{m=1}^N [Y_{nm} \cdot V_m(t) \cdot \cos(\alpha_{nm}(t))] \\ Q_n(t) = V_n(t) \cdot \sum_{m=1}^N [Y_{nm} \cdot V_m(t) \cdot \sin(\alpha_{nm}(t))] \end{cases} \quad (1)$$

where

- 1)  $P_n(t)$  and  $Q_n(t)$  are the active and reactive power injections in the  $n$ th bus at time  $t$ ;
- 2)  $\alpha_{nm}(t) = \delta_n(t) - \delta_m(t) - \theta_{nm}$ ;
- 3)  $V_n(t)$  and  $\delta_n(t)$  are the voltage magnitude and phase on the network  $n$ th bus that power flow equations are referring to;
- 4)  $V_m(t)$  and  $\delta_m(t)$  are the voltage magnitude and phase on the  $m$ th bus;
- 5)  $Y_{nm}$  and  $\theta_{nm}$  are the magnitude and phase of the admittance in the  $(n, m)$  position of the nodal admittance matrix.

#### B. EV Traffic Model

The effects of the e-mobility on the power system and the benefits of the proposed scheduling approach are evaluated by a realistic EV traffic model, reproducing the common behavior of users. In each simulation, the EV traffic is generated, over one or more days, through a stochastic approach. The main parameter to set is the penetration level of the e-mobility, i.e., the number of EVs to consider in the simulation. According

**Algorithm 1** CREATE( $\lambda_i$ )

- 1: select the base CS ( $CS_B$ ), i.e., the vehicle shelter where the car was parked during the night, from the set of all the simulated CSs (blue dots in Fig. 2; uniform distribution).
- 2:  $L_{TOT} \leftarrow$  daily journey length (normal distribution)
- 3:  $t_{DE} \leftarrow$  morning departure time from  $CS_B$  (uniform distribution)
- 4:  $t_{AR} \leftarrow$  evening arrival time to  $CS_B$  (uniform distribution)
- 5:  $N_{SO} \leftarrow$  number of stopovers throughout the day (normal distribution)
- 6:  $L_R \leftarrow L_{TOT}/(N_{SO} + 1)$  (length of each route between two CSs)
- 7:  $CS_B \leftarrow 100\%$  (charge level at the departure time)
- 8: **if**  $N_{SO} > 0$  **then**
- 9:   **for**  $n_{SO} = 1 : N_{SO}$  **do**
- 10:     stopover mean start time  $\leftarrow (t_{AR} - t_{DE}) \cdot n_{SO}/N_{SO} + t_{DE}$ .
- 11:     evaluate, based on the mean time previously calculated, the stopover actual start time (normal distribution).
- 12:     evaluate the stopover duration (normal distribution).
- 13:     **if**  $n_{SO} < N_{SO}$  **then**
- 14:       select the arrival CS from the set of CSs having a distance less than  $L_R$  from the previous one (uniform distribution).
- 15:     **else**
- 16:       select the arrival CS from the set of CSs having a distance less than  $L_R$  from the previous one and from  $CS_B$  (uniform distribution).
- 17:     **end if**
- 18:   **end for**
- 19: **end if**

to the developed model, each EV departs in the morning from a CS where it was parked overnight (Base CS:  $CS_B$ ); in the evening, the EV returns to the same station. During the day, each car travels in the city, and can stop in car parks. Car parks can be either equipped or not equipped with charge points. The EV location is unknown to the CCA until the car is plugged into a CS. As better explained in the following, in defining the path of EVs among car parks, the EV traffic model takes into account the constraints related to the distance between them. This approach allows a proper estimation of the energy consumption of EVs and of their arrival times to CSs.

The car routing behavior is defined according to a set of technical and statistical features of each EV:

- 1) capacity of EV batteries;
- 2) daily journey length, statistically defined by a normal distribution;
- 3) energy efficiency for the given path;
- 4) daily departure and arrival CS ( $CS_B$ ) (uniform distribution);
- 5) time of departure and arrival from/to each CS (uniform distribution);
- 6) number of stopovers along the day (normal distribution);
- 7) target stopover CS(s) (uniform distribution);
- 8) time window of each stopover (normal distribution).

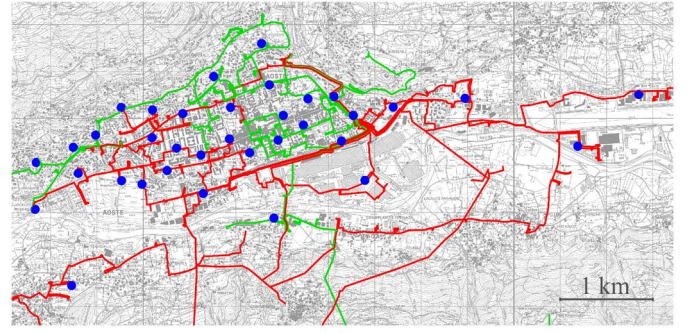


Fig. 2. MV network under study (red lines, Busbar A MV feeders; green lines, Busbar B MV feeders; and dots, CSs).

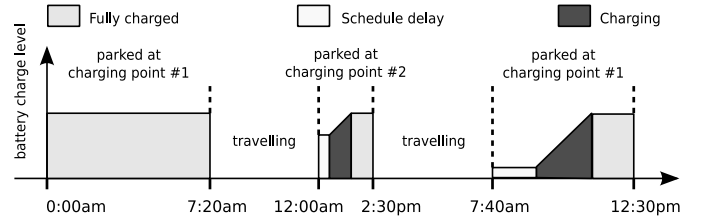


Fig. 3. Example of EV behavior, depicting its operations during one day and the corresponding battery SoC.

A specific procedure, illustrated by Algorithm 1, is performed to define the behavior of each car  $\lambda_i$ . Therefore, to simulate a population of  $N$  EVs, the algorithm is executed  $N$  times.

According to Algorithm 1, when the arrival CS is selected from the set of all the available CSs, only the CSs having a distance less than  $L_R$  from the previous one are considered. In other words, it is assumed that an EV moving from a CS to another one can travel a longer path than the shortest path available between the departure/arrival CSs (determined, in this paper, according to the Aosta city's route map). The opposite case (distance traveled by the EV shorter than the distance between the CSs) is obviously not admissible. The charge level of the EV at time  $t_{DE}$  is considered equal to 100%. Moreover, at the end of each stopover, it is assumed that the user requires the EV to be fully charged (SoC equal to 100%).

The behavior coherence of each EV is checked by suitable procedures, in order to prevent unrealistic situations (e.g., arrival time at a CS earlier than the departure time from the same CS). The simulation can be extended for the desired time horizon, e.g., several days. Using the above information, the mobility of each EV is simulated by computing its motion in the area and by tracking the batteries' SoC.

Fig. 3 shows the behavior of the car considered as an example. The EV leaves the car shelter, i.e., CS #1, at 7:20 in the morning. At departure, batteries are fully charged. Between 7:20 A.M. and 12:00 A.M., the car position is unknown to the CCA, since it is not connected to a charge point. At 12:00 A.M., the car is plugged to CS #2. The battery SoC is low, due to the distance traveled in the morning. The SoC is evaluated according to the length of the journey and the EV energy consumption per kilometer. The CCA considers the stopover time selected by the user (until 2:30 P.M.) and the

grid needs to determine the schedule of the charging process. The operation is delayed to limit the peak of the energy flows on the grid and to prevent violations of voltage and current limits. At 2:30 P.M. the car leaves the CS #2. At 7:40 P.M., the EV returns to the CS #1, where its SoC is fully restored overnight.

### C. EV Energy Model

From the power grid perspective, the EV is seen as a load that can be plugged in any available CS. For the purpose of the scheduling algorithm, an EV is modeled as follows. At time  $t$ , a set of  $H(t)$  EVs is connected to the electrical grid. The set of connected EVs is denoted with  $\Lambda(t) = \{\lambda_1, \dots, \lambda_{H(t)}\}$ . The SoC of the battery of  $\lambda_i$  EV at time  $t$  is denoted with  $\gamma_i(t)$ , expressed in [kWh]. Vehicle  $\lambda_i$  is plugged to a CS at the request time  $r_i$ . The SoC at time  $r_i$  is thus  $\gamma_i(r_i)$ . When the EV is plugged to the CS, a relative deadline  $D_i$  is set by the user. The battery needs to be recharged up to a minimum threshold  $\gamma_i^{th}$  before the absolute deadline  $d_i = r_i + D_i$ . Therefore, it must hold  $\gamma_i(d_i) \geq \gamma_i^{th}$ .

The charge of all EVs connected to the power grid is controlled by the CCA. The time is discretized in units having duration equal to  $\tau$ , expressed in [h] (e.g.,  $\tau = 0.25$  h or  $\tau = 1$  h). Formally, the CCA assigns a schedule to each EV  $\lambda_i \in \Lambda(t)$ , modeled by the function  $s_i(t) : \mathbb{N}_0 \rightarrow \{0, 1\}$

$$s_i(t) = \begin{cases} 1 & \text{if load } \lambda_i \text{ is charging at time } t \\ 0 & \text{otherwise.} \end{cases} \quad (2)$$

The  $\lambda_i$  EV is assumed to absorb a total amount of power equal to  $P_i$  (expressed in [kW]) while charging. The number of time units required to charge the  $\lambda_i$  EV can be calculated as

$$C_i = \left\lceil \frac{\gamma_i^{th} - \gamma_i(r_i)}{P_i \cdot \tau} \right\rceil. \quad (3)$$

More refined models can be used to estimate the required charge time [29], [30]. However, for the sake of simplicity, we adopt the model leading to (3), which assumes a constant charging rate ( $P_i$ ) during the whole charging period. Such a model is correspondent with the actual commercially available technologies.

## V. SCHEDULING OF CHARGING PROCESSES

The CCA allocates the CRs of users in time to optimize the efficiency of the grid operation and to prevent violations of the relevant technical constraints. A charging process is considered nonpreemptable: this means that, once started, it can not be stopped and resumed later. This policy corresponds to the one actually in place in the Italian scenario, nevertheless, it reduces the overall efficiency of the scheduler. In fact, for instance, an ongoing charging process with a long deadline cannot be stopped and delayed in favor of a charging process having a shorter deadline. On the other hand, repeated partial charging cycles can negatively affect the battery efficiency and duration. Nonpreemptable CRs prevent these issues.

The first step, as depicted in Fig. 1, consists in the acquisition of the overall active power demand forecast affecting the

---

### Algorithm 2 ALLOCATE( $\lambda_i$ )

---

- 1: calculate  $C_i$  using (3)
  - 2: select the best starting time  $\sigma_{\text{best}}$  that satisfies (4) and (8)
  - 3: evaluate the power flow on  $A_{\text{best}} = [\sigma_{\text{best}}, \sigma_{\text{best}} + C_i]$  considering the allocated  $\lambda_i$
  - 4: **if** power constraints are satisfied within  $A_{\text{best}}$  **then**
  - 5:   allocate  $\lambda_i$  starting from  $\sigma_{\text{best}}$
  - 6: **else**
  - 7:   evaluate the power flow on  $[r_i, d_i] \rightarrow f_i(t)$
  - 8:   find the set  $\Sigma'_i$  as defined in (12)
  - 9:   **if**  $\Sigma'_i = \emptyset$  **then**
  - 10:     car  $\lambda_i$  not schedulable
  - 11:   **else**
  - 12:     select the best starting time  $\sigma_{\text{best}} \in \Sigma'_i$  using (8)
  - 13:     allocate  $\lambda_i$  starting from  $\sigma_{\text{best}}$
  - 14:   **end if**
  - 15: **end if**
- 

distribution grid. Such acquisition assumes that suitable historical data and forecasting models (see [31]) are available as an external source of information with respect to the method described in this paper. The time horizon of the forecast must be chosen suitably: the CCA will optimize the EVs' CRs according to the grid's requirements along this time interval. For example, a 24 h prediction could be an adequate trade-off between flexibility of the scheduling process and forecasting accuracy. The power profile is updated when new forecasts are available (e.g., every hour). The power demand forecasting is a key issue for the performance of the optimization process, due to the limited information usually available to the DSO. In this paper, from this viewpoint, a short-term future scenario is considered, i.e., a MV network with monitoring systems able to acquire suitable data on MV feeders, MV/LV substations, users, and CSs. Although this is not yet the most commonly adopted solution by DSOs, some real-life implementations can already be found [32] and their massive deployment is expected in the near future [33]. Concerning the time requirements on data collection and processing, it is important to point out that, as previously explained, the CCA schedules the EVs according to the forecasted behavior of the network (e.g., 24 h in advance); therefore, the data collection on the grid does not need to be accomplished strictly in real-time (e.g., the refresh of the forecasting could be performed once per hour). At time  $t$ , the power profile is modeled by the function  $p : \mathbb{N}_0 \rightarrow \mathbb{R}$ .

When a new EV  $\lambda_i$  is connected to a CS, the CCA gathers the information detailed in Section III. Algorithm 2 is executed to allocate the CR submitted by  $\lambda_i$ . First, the time required to charge the battery up to the desired SoC is evaluated using (3). Afterwards, the algorithm computes the set  $\Sigma_i$ , which is composed by all the possible suitable time instants to start the charging process. Formally, this set is defined as

$$\Sigma_i = \{\sigma : \forall \sigma \in \mathbb{N}_0 : r_i \leq \sigma \leq d_i - C_i\} \quad (4)$$

where  $d_i = r_i + D_i$  is referred as absolute deadline.

For each time  $\sigma_k \in \Sigma_i$ , the CCA computes the two values  $\bar{p}_k$  and  $\hat{p}_k$  as follows:

$$\bar{p}_k = \frac{1}{C_i} \cdot \sum_{t=\sigma_k}^{\sigma_k+C_i} p(t) \quad \sigma_k \in \Sigma_i \quad (5)$$

$$\hat{p}_k = \max_{t \in [\sigma_k, \sigma_k+C_i]} p(t) \quad \sigma_k \in \Sigma_i. \quad (6)$$

While  $\bar{p}_k$  represents the average power consumption in the time interval  $[\sigma_k, \sigma_k+C_i]$ ,  $\hat{p}_k$  is the greatest power consumption in the same interval.

The CCA uses a ‘‘valley filling’’ approach to determine the best candidate starting time  $\sigma_{\text{best}}$ . The scheduler computes

$$\Sigma_i^{\min} = \{\sigma_m \in \Sigma_i : m = \operatorname{argmin} \bar{p}_k\} \quad (7)$$

and the algorithm chooses

$$\sigma_{\text{best}} = \sigma_m \in \Sigma_i^{\min} : m = \operatorname{argmin} \hat{p}_k. \quad (8)$$

Afterwards, the power-flow procedure is evaluated on the time interval  $[\sigma_{\text{best}}, \sigma_{\text{best}}+C_i]$ . For all time slots  $t$  of the considered interval, the power flow determines the power exchanges in all buses of the network. For the generic  $n$ th bus, these are equal to

$$\begin{cases} P_j(t) = - \sum_{i=1}^{h_j(t)} P_i(t) - P_{L_j}(t) + P_{G_j}(t) \\ Q_j(t) = -Q_{L_j}(t) + Q_{G_j}(t). \end{cases} \quad (9)$$

$P_{L_j}(t)$  and  $Q_{L_j}(t)$  are, respectively, the active and reactive withdrawals of the load subtended to the  $j$ th bus.  $P_{G_j}(t)$  and  $Q_{G_j}(t)$  are the DG injections in the  $j$ th bus, if any.  $\sum_{i=1}^{h_j(t)} P_i(t)$  is the power absorbed by the  $h_j(t)$  cars currently charging in the  $j$ th bus. The power-flow procedure uses the values assessed by (9) to solve (1). The solution of such equations provides the voltages  $[\bar{V}(t)]$ . The currents flowing in every branch of the grid are evaluated as

$$[\bar{I}(t)] = [\bar{Y}] \cdot [\bar{V}(t)]. \quad (10)$$

$[\bar{V}(t)]$  and  $[\bar{I}(t)]$  are used to check the electrical constraints on voltages and currents.

The execution of the power-flow procedure could be time-consuming. The computation time depends on the length of the considered time interval. The adopted approach reduces the timespan where the power flow is evaluated, improving the computational performance of the algorithm. If all power constraints are satisfied within the examined time frame, then the charge of  $\lambda_i$  EV is allocated at time  $\sigma_{\text{best}}$ . Otherwise, the charge in the interval  $[\sigma_{\text{best}}, \sigma_{\text{best}} + C_i]$  is not feasible. In order to find another valid interval, the CCA has to evaluate the whole time period  $[r_i, d_i]$  to check for violations. The power-flow computes the function  $f_i : \mathbb{N}_0 \rightarrow \{0, 1\}$

$$f_i(t) = \begin{cases} 1 & \text{if load } \lambda_i \text{ does not cause violations at time } t \\ 0 & \text{otherwise.} \end{cases} \quad (11)$$

Based on this function, the CCA calculates the following set:

$$\Sigma'_i = \{\sigma \mid r_i \leq \sigma \leq d_i - C_i \wedge f_i(t) = 1 \quad \forall t \in [\sigma, \sigma + C_i]\}. \quad (12)$$

The set is composed by candidates starting times of intervals suitable for the charge, i.e., those generating no violations of electrical constraints. If this set is empty, then the EV is not schedulable. Otherwise, for each  $\sigma_k$  in  $\Sigma'_i$ , the CCA computes the values of  $\bar{p}_k$  and  $\hat{p}_k$  using (5) and (6) and chooses the interval  $[\sigma_{\text{best}}, \sigma_{\text{best}} + C_i]$  using (7) and (8). If the algorithm terminates successfully, then the functions  $s_i(t)$  and  $p(t)$  are updated considering the newly allocated EV.

The proposed approach can suitably deal with a low accuracy in the power demand forecast. In case of significant discrepancy between forecasted and actual overall power demand, the same algorithm can be applied to reschedule all the CRs currently scheduled to start in the future. The tolerance against forecasting approximations is thus considered a design parameter that can be tuned according to the power network characteristics. The rescheduling process is not applied to currently charging EVs since it is assumed that charging processes are not interruptible. The reallocation of all reschedulable EVs is feasible in practice due to the low per-car computational time assessed in Section VII: approximately 45 s are required to reschedule 1000 EVs, using a common personal computer (see Section VII). According to previous assumptions, this operation shall be performed when fresh information regarding the power demand is gathered, e.g., once per hour. On the other hand, in case of critical working conditions of the power infrastructure, current charging processes can be stopped upon request. A new schedule can be generated after the critical condition has elapsed.

## VI. NUMERICAL ANALYSES

The performance assessment of the proposed scheduling approach is carried out by means of numerical simulations based on a real distribution network. Three scenarios are implemented and compared.

- 1) *No CCA–No Technical Limits (noCCA–noTL)*: In this scenario, no CCA is used to manage EVs’ CRs. Therefore, battery charging starts when the user plugs the car into a CS. Moreover, an ideal grid is assumed, i.e., a network able to accept all the EV CRs. This case is simulated for comparison purposes: it represents the best possible condition that could be achieved by adequate investments on network development.
- 2) *No CCA–Technical Limits (noCCA–TL)*: This is the reference scenario (existing system). As above, no scheduling operations are performed. The DSO sheds the load if needed, by inhibiting EVs charging during grid overloads.
- 3) *CCA–Technical Limits (CCA–TL)*: The EV charging is managed by our proposed CCA to improve the grid operation (avoid overloads and efficiency lowering) and to achieve user requests regarding the desired charging time (i.e., deadlines).

The analysis is carried out with different EV penetration levels. The number of simulated EVs ranges from 1000 up to 20 000 in steps of 1000 EVs. Since each EV may require more than one charge during the simulation time, the number of CRs (i.e., the workload) is usually higher than the total number of

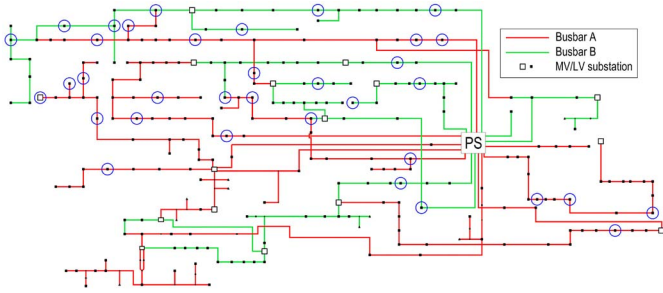


Fig. 4. Single line diagram of the electrical grid under study.

TABLE I  
NETWORK INFORMATION

Busbars	Feeder	LV users		MV users		MV active users	
		Number [n°]	Rated power [MW]	Number [n°]	Rated power [MW]	Number [n°]	Rated power [MW]
A	1	3,211	5.670	1	0.081	0	0
	2	2,366	5.453	6	1.598	0	0
	3	2,067	2.170	3	0.440	1	0.015
	4	1,172	5.030	8	1.557	0	0
	5	1,522	2.990	7	2.679	0	0
	6	299	2.255	13	5.637	1	1.815
	7	1,739	5.700	5	1.060	0	0
	8	451	0.910	1	0.188	0	0
	9	3,417	0.470	1	0.155	0	0
B	1	2,168	5.003	4	0.684	1	0.190
	2	2,355	5.870	2	0.345	0	0
	3	529	0.920	2	0.432	0	0
	4	0	0	2	0.013	2	2.620
	5	4,384	6.720	1	0.010	0	0
	6	2,238	3.740	2	1.636	0	0
	7	1,502	3.430	5	0.574	0	0

EVs. Under different workloads, the simulation evaluates the grid operational efficiency, the scheduling process efficacy, and the customer satisfaction (full charge accomplished within the desired deadline).

For each EV penetration level, 30 different simulation runs are performed. This number of attempts is a suitable trade-off between degree of convergence of results and computational effort. Each run is carried out on a time horizon of three days. However, only the results relevant to the central day are considered in our statistical analysis. The first and the third day are simulated to avoid side effects on variables, which could occur at the boundaries of the time interval.

#### A. Network Under Study

The network under study, operated by an Italian distribution company named DEVAL [34], supplies the city center and the neighborhood of Aosta, the chief town (population of 35 000 inhabitants) of the Valle d'Aosta region, in the Northwest of Italy.

The MV network has a radial structure, starting from a HV/MV primary substation equipped with two 132/15 kV transformers, each one rated 25 MVA (Figs. 2 and 4). Each grid, underlying a MV busbar (in the following, called network A and B), acts independently of the other. Both networks are modeled since the EV traffic in Aosta city affects the operation of the entire distribution grid: at different instants, EVs can be connected to networks A or B according to their motion within the city. Networks A and B have 9 and 7 feeders, respectively. Table I provides additional technical information about the network load and DG.

The considered scenario refers to an urban area in a mountain region. Therefore, the DG penetration is rather small:

five power plants (3 CHP, 1 photovoltaic, and 1 hydro) are connected to the MV grid. Power injections of LV power plants (mainly photovoltaic) are negligible. The grid model is implemented in MATLAB, by using function libraries derived from the MATPOWER package [35]. All energy flows in the grid are represented on an hourly basis, according to the time resolution adopted by DEVAL to measure the energy exchanges of the MV/LV users of Aosta. In compliance with the Italian regulation, all MV users are subject to a hourly assessment of their power demand (on the other hand, smaller users are monitored according to peak/off-peak time bands).

Each MV active/passive user has a specific exchange profile (obtained by on-field measurements), while all LV users are assumed to have the same withdrawal characteristic, obtained from the residual energy exchange profile at the HV/MV interface scaled according to the rated power of each user (energetic equivalence between the actually measured energy flows and their estimation).

It is supposed that 35 CSs are installed in the grid. Their location has been defined by considering the following factors:

- 1) closeness to the city center, to residential and industrial districts, or the other points of interest for users (e.g., the airport area);
- 2) proximity to existing MV feeders;
- 3) presence of parking lots or squares;
- 4) information about the local DEVAL projects for the deployment of the e-mobility infrastructure in the urban area of Aosta [36].

It is supposed that all the CSs are connected at MV level. No constraints are imposed on the number of simultaneously pluggable EVs in each station. This assumption is adopted to highlight the technical limits of the network and not those of the e-mobility infrastructure, which we assume suitably sized according to the actual users needs.

Concerning the electrical grid, the following technical limits have been considered. With respect to voltage profiles, EN 50160 [37] states that every bus of MV/LV networks must be kept within the  $\pm 10\%$  of rated voltage. In this paper, MV voltages are assumed acceptable if included between 96% and 110%. The inferior limit is set to 96% to accommodate voltage drops on the LV network. The transit limit is set to 80% of the rated ampacity of conductors and HV/MV transformers, in order to avoid an excessive aging of components and a reduction in energy transport efficiency. As a simplifying assumption, all EVs are modeled with the same technical parameters. Power withdrawal  $P_i$  is 20 kW [38]; it is assumed constant during the whole charging process. Three-phased chargers connected to a balanced system are considered in the analysis. Battery capacity is 40 kWh [38]. Energy consumption of the car during use is constant at 0.2 kWh/km. This value is compliant with data declared in [39] and, for the particular scenario into analysis, is assessed by experimental measurements obtained in an e-mobility research project performed in the Aosta area [36].

The car behavior is defined according to statistical parameters. Such parameters have been identified from the information collected in real life applications (these data were collected on the DEVAL car fleet, over the year 2011, and

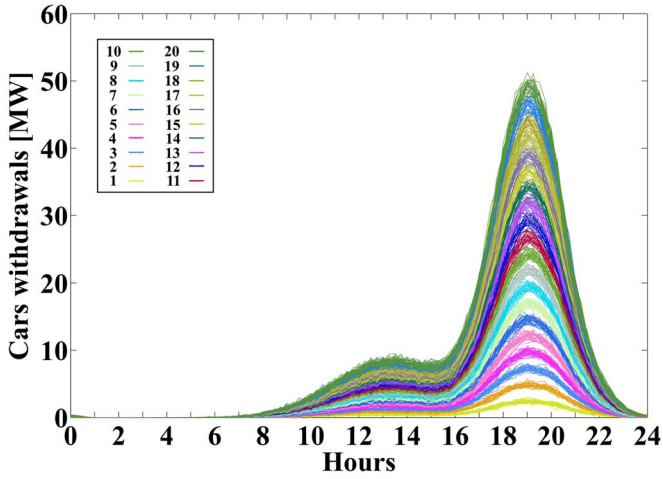


Fig. 5. Daily load profile due to e-mobility in Aosta. Different curves refer to different number of EVs (thousands of EVs).

on statistical surveys on the Italian automotive scenario). The adopted parameters are not meant to depict a specific case study: they are defined to enable the simulation of a realistic scenario (i.e., the management of the e-mobility load requirements in a typical medium-sized urban area in Italy), useful to assess the performance of the proposed algorithm. The following parameters/values have been used.

- 1) Daily journey length:  $\mu = 39.02$  km,  $\sigma = 10.99$  km, minimum value = 10 km [40].
- 2) Departure time from the  $CS_B$ :  $\mu = 7$  A.M.,  $\sigma = 1.5$  h.
- 3) Arrival time to the  $CS_B$ :  $\mu = 7$  P.M.,  $\sigma = 1.5$  h.
- 4) Number of stopovers throughout the day:  $\mu = 0$ ,  $\sigma = 1$ .
- 5) Start time of each stopover:  $\mu$  of each stopover equally spaced on the interval between the departure and arrival time from/to the  $CS_B$ ,  $\sigma = 1.5$  h.
- 6) Duration of each stopover:  $\mu = 0$ ,  $\sigma = 0.3$  h.

Fig. 5 shows the daily load profile generated by Algorithm 1 while using the above parameters.

It is worth noting that the load characteristic is compliant with the findings of the literature on the future impact of EVs on electric power systems [41], [42].

### B. Assessment of Benefits on Grid Operation

First, the quality of service guaranteed to users is discussed. This factor is related to the number of CRs rejected due to technical limitations and electrical constraints.

Fig. 6 reports the average number of CRs that are satisfied in the 3 simulated scenarios. For each level of EV penetration, the errorbars indicate the minimum and maximum values assessed over 30 simulation runs.

The beneficial effect of the CCA scheduling increases with the EV penetration level. When up to 3000 EVs are simulated, the number of CRs per day ranges in the interval [4000, 10000]. In this case, the grid is always able to satisfy all the CRs (same results in noCCA-TL and CCA-TL scenarios). If the EVs population grows, the energy flows generated by EVs charges can cause violations of the grid electrical constraints. Without scheduling actions, some CRs must be rejected to preserve the good functioning of the grid

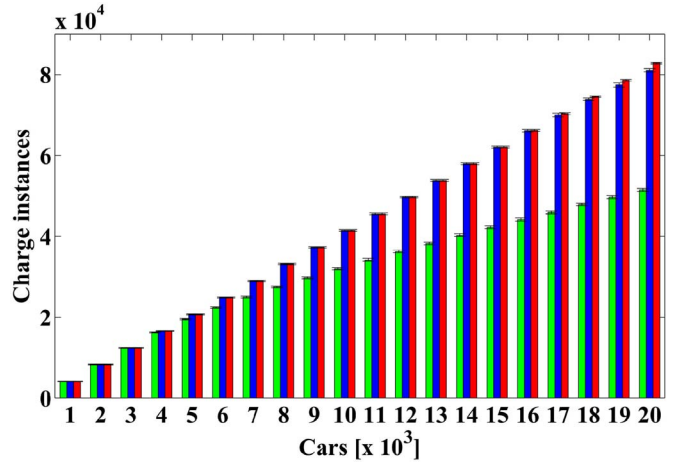


Fig. 6. CRs accepted in the EVs' scenarios. The green bar refers to noCCA-TL, the blue bar to CCA-TL, and the red to the noCCA-noTL scenario.

(instances accepted in the noCCA-TL scenario less than in the noCCA-noTL scenario). On the other hand, in the CCA-TL scenario, the CCA postpones EV CRs (according to the deadlines imposed by users) in order to avoid the network overload and to better fulfill users needs. In particular, in this case, with a population between 4000 and 15000 EVs all the CRs are satisfied. For example, with 15000 EVs (equivalent to about 60000 CRs) nearly 33% of CRs are rejected without CCA. If the EV population rises further, some CRs are also rejected in the CCA-TL scenario. For example, considering a population of 20000 EVs (about 80000 CRs), the CCA rejects about 2.14% of CRs, while in the noCCA-TL scenario about 38% of CRs is rejected.

For all the considered EV penetration levels (from 1000 to 20000 EVs), Fig. 7(a) and (b) shows the daily power absorption profile due to the EV load only, in the noCCA-TL and CCA-TL scenarios, respectively. In the noCCA-TL case, when the e-mobility penetration is above 4000 EVs, the load requirements can lead to overload conditions on the grid (violations of transit and voltage limits), especially in the evening. For example, with 20000 EVs, the uncoordinated EV charging would bring to a peak load of 50 MW in the absence of adequate counter-measures. This is the theoretical peak load achieved in the noCCA-noTL scenario, reported in Fig. 5. In real-life conditions, the grid of Aosta is able to accept an EV load equal to, or lower than, about 18 MW. This fact can be deduced by observing Fig. 7(a) and (b): the results highlight that the CRs causing the power load to exceed 18 MW are rejected [noCCA-TL case in Fig. 7(a)] or delayed by the CCA [CCA-TL scenario depicted in Fig. 7(b)]. In the first case, the quality of service provided to users is negatively affected. Conversely, using the CCA, the nighttime is exploited (in compliance with the deadlines set by users) to smooth the energy exchanges at the HV/MV interface and to avoid the violation of the network technical constraints.

The actual peak shaving action performed by the CCA is illustrated in Fig. 8. The behavior represents the impact of the energy flows on MV lines. Fig. 8(a) shows the daily profile of the active power at the HV/MV interface of the distribution

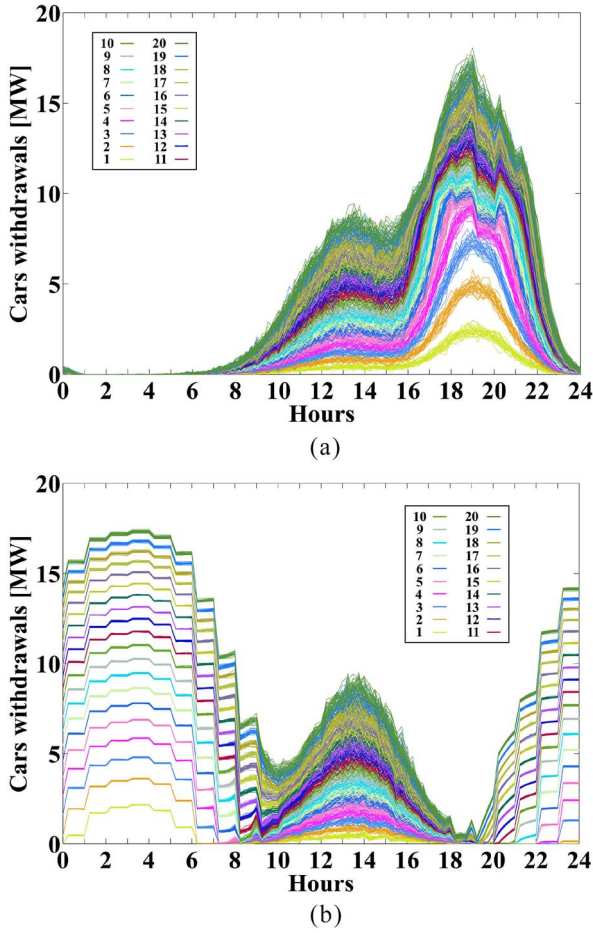


Fig. 7. Daily power demand profile of EVs (a) with CCA and (b) without CCA.

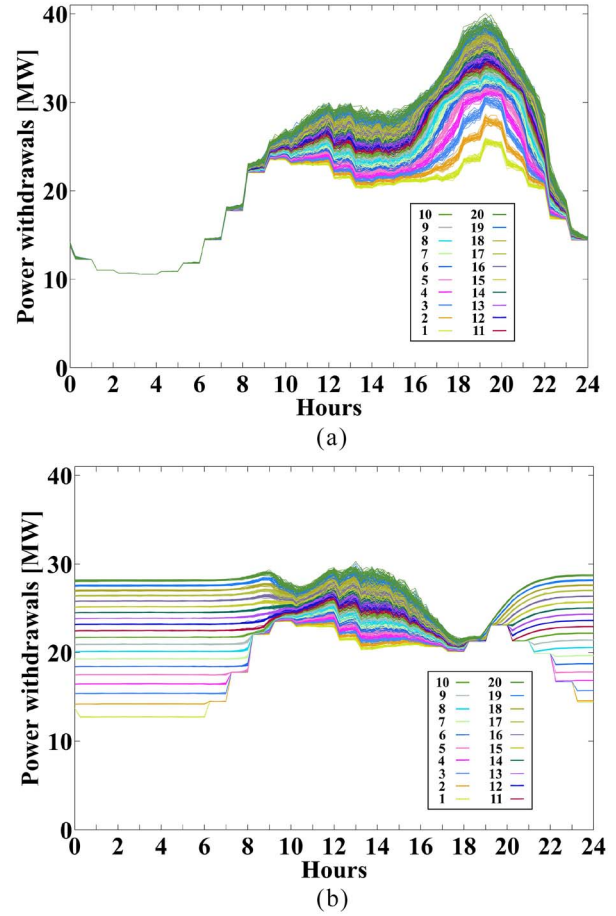


Fig. 8. Daily power demand measured at the HV/MV interface of the network (a) without CCA and (b) with CCA.

network in the noCCA-TL scenario, considering the energy load of only the EVs actually charged. Fig. 8(b) reports the same quantity in the CCA-TL scenario. The scheduling action provides a clear improvement on the peak load. For example, in the 20 000 EVs scenario, the daily peak in the noCCA-TL case is about 40 MW, while in the CCA-TL case it is lower than 30 MW.

Fig. 9 shows the improvement of the network operation efficiency achievable by the CCA. The plot reports the daily energy losses in the MV conductors and HV/MV transformers according to the EV penetration in the grid, in the three scenarios considered. The CCA-TL scenario presents higher losses with respect to the noCCA-TL case. However, this is due to the higher number of CRs that are satisfied. A better comparison can be performed between the CCA-TL and noCCA-noTL cases (almost the same number of EV CRs satisfied). As reported in Fig. 9, the efficiency begins to appreciably improve at low EV penetration levels (between 1000 and 4000 cars). It further increases with the increase of the energy flows on the network. For example, let us consider the case with 20 000 EVs. The CCA-TL scenario accepts 97.9% of CRs (81 057 in Fig. 6). Losses are 6.05 MWh/day, which is 67.3% of noCCA-noTL losses. In the noCCA-TL scenario, only 37.9% of EV CRs are satisfied. In this case, energy losses are 4.8 MWh/day, which is 53.3% of noCCA-noTL losses.

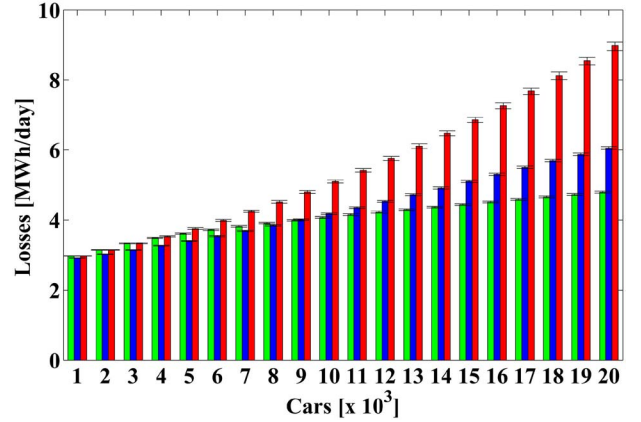


Fig. 9. Energy losses in grid conductors and HV/MV transformers in the EV scenarios. The green bar refers to noCCA-TL, the blue bar to CCA-TL, and the red bar to the noCCA-noTL scenario.

## VII. COMPUTATIONAL PERFORMANCE

This section provides an analysis of the computational performance of the proposed algorithm. The overall performance is determined by the performance of the two involved procedures, i.e., the evaluation of the grid's constraints and the allocation of the charging process at the proper time instant. The computational complexity of the first procedure, which

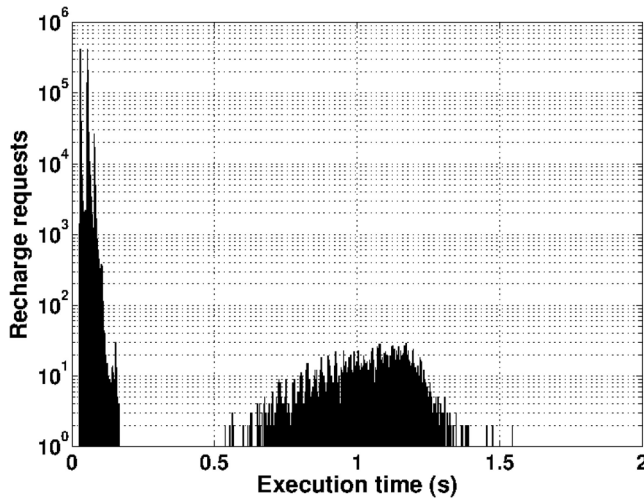


Fig. 10. Distribution of the time required to evaluate CRs. The vertical axis has a logarithmic scale.

requires load flow analyses, grows with the size of the power network [43]. The bottleneck of the load flow analysis consists in the inversion of the  $[\bar{Y}]$  matrix [see (10)], which is an  $N \times N$  matrix, where  $N$  is the number of buses in the network. This operation can be performed in  $O(N^3)$  using the Gaussian elimination method [44]. On the other hand, the complexity of the allocation procedure is  $O(D_i)$  for the  $\lambda_i$  EV. In fact, (4)–(8) are evaluated sequentially, and each of them can be computed in linear time with respect to  $D_i$ . Therefore, the time required for the allocation procedure does not depend on the network size.

The histogram in Fig. 10 shows the distribution of the execution time required to evaluate each CR. The plot presents the measurements of 32 simulations in case of 15 000 EVs. It uses a logarithmic scale for the vertical axis to suitably depict the details of the distribution. With this level of EV penetration, all the parts of the scheduling algorithm are executed. This fact allows a complete evaluation of its computational performance.

The simulation was run on a computer equipped with an Intel Core i7-2630QM, 8 GiB of RAM, a Linux operating system with kernel 3.2.0 and MATLAB version 7.10.0.499 (R2010a). The average execution time of the algorithm is 0.047 s. The distribution is characterized by two separated sets of results. The first set presents a maximum execution time slightly less than 0.2 s. These CRs are related to EVs connected to the grid when the system load is sufficiently low. Its average execution time is close to 0.045 s. 99.7% of CRs are contained in this set. The CRs result to be completely evaluated at line 5 of Algorithm 2. The second set encompasses CRs requiring the complete execution of Algorithm 2. The execution time of this set is upper bounded by 1.55 s. Given the described results, the short execution time required by scheduling process allows a real-time evaluation of CRs.

## VIII. CONCLUSION

This paper presented a method to coordinate the charge of EVs based on a scheduling approach. The proposed strategy

performs the peak shaving of the power demand profile caused by EVs CRs. Technical constraints of the distribution infrastructure are guaranteed by the integrated load flow analysis, while the quality of service provided to users is preserved (the EV charge is postponed in compliance with the deadline set by the user). The application of the proposed method to an existing power network has shown, in scenarios with a considerable penetration of the e-mobility, a peak load reduction by 25%. Reduced peak loads allow the DSO to postpone investments needed for the network development due to the rising of e-mobility, improving the exploitation of distribution assets and generating capacity. Moreover, energy losses are significantly reduced (from  $-53\%$  to  $-63\%$ , depending on the scenario). Finally, the scheduling of CRs is performed in real-time: the average computation time required for the allocation of each charging process is 45 ms, while the longest computation time is around 1.5 s. This performance refers to the grid mathematical model implemented in the electric grid's control center of the city of Aosta (managed by the local DSO, DEVAL), i.e., this paper proposed corresponds to a real-life application.

## ACKNOWLEDGMENT

The authors would like to thank DEVAL SpA for the support provided.

## REFERENCES

- [1] *Laying the Foundations for Greener Transport—TERM 2011: Transport Indicators Tracking Progress Towards Environmental Targets in Europe*, Office Off. Publ. Eur. Union, Eur. Environ. Agency, Luxembourg, EEA Rep. 7/2011.
- [2] *Roadmap to a Single European Transport Area—Towards a Competitive and Resource Efficient Transport System*, Eur. Comm., Brussels, Belgium, 2011.
- [3] *Europe's cars? An Analysis of Carmaker Progress Towards EU CO2 Targets in 2009*, Eur. Fed. Transport Environ., Brussels, Belgium, 2011.
- [4] (Apr. 2013). *Global EV Outlook, Understanding the Electric Vehicle Landscape to 2020*, International Energy Agency. [Online]. Available: <http://www.iea.org/publications/freepublications/publication/global-evoutlook.html>
- [5] UBS, Global Research. (Aug. 2014). *Will Solar, Batteries and Electric Cars Re-Shape the Electricity System?* [Online]. Available: <https://neo.ubs.com/#article/research/ues45625>
- [6] ANSA. (Oct. 2014). *Italia Paese a Maggior Densità automobilistica in Europa*. [Online]. Available: [http://www.ansa.it/motori/notizie/rubriche/analisiapprofondimenti/2012/06/13/Auto-Italia-paese-maggior-densita-circolante-Europa\\_7030670.html](http://www.ansa.it/motori/notizie/rubriche/analisiapprofondimenti/2012/06/13/Auto-Italia-paese-maggior-densita-circolante-Europa_7030670.html)
- [7] *The Drive Towards Smart Grids: A Fact Sheet by the European Energy Regulators on How the Drive Towards Smarter Grids can Help Meet European Policy Objectives on Energy and Climate Change and Empower Customers*, Council Eur. Energy Reg. (CEER), Eur. Reg. Group Electricity Gas (ERGEG), Brussels, Belgium, Oct. 2010.
- [8] L. Pieltain Fernández, T. Román, R. Cossent, C. Domingo, and P. Frías, "Assessment of the impact of plug-in electric vehicles on distribution networks," *IEEE Trans. Power Syst.*, vol. 26, no. 1, pp. 206–213, Feb. 2011.
- [9] S. Shafiee, M. Fotuhi-Firuzabad, and M. Rastegar, "Investigating the impacts of plug-in hybrid electric vehicles on power distribution systems," *IEEE Trans. Smart Grid*, vol. 4, no. 3, pp. 1351–1360, Sep. 2013.
- [10] *Italian Legislative Decree 16 March 1999, n. 79, Application of Directive 96/92/CE, Containing Common Regulations for the Internal Market of the Electricity*, Italian Parliament, Rome, Italy, Mar. 1999.
- [11] (2008). *Code for the Terms and Conditions for Electricity Grid Connection With the Obligation to Connect Third Party Electricity Generation Plants (Code for Active Connections—TICA)*. [Online]. Available: <http://www.autorita.energia.it>

- [12] M. H. J. Bollen and M. Häger, "Power quality: Interaction between distributed generation, the grid and other customers," *Elect. Power Qual. Utilisation Mag.*, vol. 1, no. 1, pp. 51–61, 2005.
- [13] J. Deuse *et al.*, "Interactions of dispersed energy resources with power system in normal and emergency conditions," in *Proc. CIGRE Int. Conf. Large Elect. Syst.*, Paris, France, 2006, pp. 1–12.
- [14] D. Bertini *et al.*, "Hosting capacity of Italian LV distribution networks," in *Proc. 21th Int. Conf. Elect. Distrib. (CIRED)*, Frankfurt, Germany, Jun. 2011, Art. ID 0930.
- [15] C. W. Taylor, *Power System Voltage Stability* (EPRI Power System Engineering Series). New York, NY, USA: McGraw Hill, 1994.
- [16] M. Merlo, N. Scordino, and F. Zanellini, "Optimal power flow approach to manage dispersed generation rise and passive load energy needs over a distribution grid," *Int. Rev. Elect. Eng.*, vol. 8, no. 5, pp. 1482–1494, 2013.
- [17] O. Sundstrom and C. Binding, "Flexible charging optimization for electric vehicles considering distribution grid constraints," *IEEE Trans. Smart Grid*, vol. 3, no. 1, pp. 26–37, Mar. 2012.
- [18] K. De Craemer, S. Vandael, B. Claessens, and G. Deconinck, "An event-driven dual coordination mechanism for demand side management of PHEVs," *IEEE Trans. Smart Grid*, vol. 5, no. 2, pp. 751–760, Jul. 2013.
- [19] Y. He, B. Venkatesh, and L. Guan, "Optimal scheduling for charging and discharging of electric vehicles," *IEEE Trans. Smart Grid*, vol. 3, no. 3, pp. 1095–1105, Sep. 2012.
- [20] E. Sortomme and M. El-Sharkawi, "Optimal scheduling of vehicle-to-grid energy and ancillary services," *IEEE Trans. Smart Grid*, vol. 3, no. 1, pp. 351–359, Mar. 2012.
- [21] A. Al-Awami and E. Sortomme, "Coordinating vehicle-to-grid services with energy trading," *IEEE Trans. Smart Grid*, vol. 3, no. 1, pp. 453–462, Mar. 2012.
- [22] J. Soares, H. Morais, T. Sousa, Z. Vale, and P. Faria, "Day-ahead resource scheduling including demand response for electric vehicles," *IEEE Trans. Smart Grid*, vol. 4, no. 1, pp. 596–605, Mar. 2013.
- [23] S. Deilami, A. Masoum, P. Moses, and M. A. S. Masoum, "Real-time coordination of plug-in electric vehicle charging in smart grids to minimize power losses and improve voltage profile," *IEEE Trans. Smart Grid*, vol. 2, no. 3, pp. 456–467, Sep. 2011.
- [24] Z. Fan, "A distributed demand response algorithm and its application to PHEV charging in smart grids," *IEEE Trans. Smart Grid*, vol. 3, no. 3, pp. 1280–1290, Sep. 2012.
- [25] A. Di Giorgio, F. Liberati, and S. Canale, "Electric vehicles charging control in a smart grid: A model predictive control approach," *Control Eng. Pract.*, vol. 22, no. 1, pp. 147–162, 2014.
- [26] S. Bashash and H. Fathy, "Robust demand-side plug-in electric vehicle load control for renewable energy management," in *Proc. Amer. Control Conf. (ACC)*, San Francisco, CA, USA, Jun. 2011, pp. 929–934.
- [27] G. Benetti *et al.*, "Management of electric vehicles charging processes in a DSO control center," in *Proc. Chall. Implement. Active Distrib. Syst. Manage. (CIRED)*, Rome, Italy, Jun. 2014, Art. ID 0401.
- [28] *Reference Technical Rules for the Connection of Active and Passive Consumers to the HV and MV Electrical Networks of Distribution Company*, CEI Standard CEI 0-16, Dec. 2013.
- [29] J. Álvarez Antón *et al.*, "Battery state-of-charge estimator using the MARS technique," *IEEE Trans. Power Electron.*, vol. 28, no. 8, pp. 3798–3805, Aug. 2013.
- [30] L. Lam and P. Bauer, "Practical capacity fading model for Li-ion battery cells in electric vehicles," *IEEE Trans. Power Electron.*, vol. 28, no. 12, pp. 5910–5918, Dec. 2013.
- [31] J. Tailor and R. Buizza, "Neural network load forecasting with weather ensemble predictions," *IEEE Trans. Power Syst.*, vol. 17, no. 3, pp. 626–632, Aug. 2002.
- [32] D. Delfanti, D. Falabretti, F. Fiori, and M. Merlo, "Smart grid on field application in the Italian framework: The A.S.S.E.M. project," *Elect. Power Syst. Res.*, to be published.
- [33] Grid4EU. (2014, Oct.). *Official Web Site*. [Online]. Available: <http://www.grid4eu.eu/>
- [34] (2013). *Deval SpA*. [Online]. Available: <http://www.devalspa.it/>
- [35] R. Zimmerman, C. Murillo-Sánchez, and R. Thomas, "MATPOWER: Steady-state operations, planning and analysis tools for power systems research and education," *IEEE Trans. Power Syst.*, vol. 26, no. 1, pp. 12–19, Feb. 2011.
- [36] Rê. V. E. Grand Paradis. (Oct. 2014). *Official Web Site*. [Online]. Available: <http://www.grand-paradis.it/progetti/647-reve-grand-paradis>
- [37] *Voltage Characteristics of Electricity Supplied by Public Distribution Networks*, CEI Standard CEI EN 50160, May 2011.
- [38] R. Garcia-Valle and J. P. Lopes, *Electric Vehicle Integration into Modern Networks*. New York, NY, USA: Springer, 2013.
- [39] International Transport Forum. (Apr. 2012). *Electric Vehicles Revisited—Costs, Subsidies and Prospects*. [Online]. Available: <http://www.internationaltransportforum.org/jtrc/DiscussionPapers/DP201203.pdf>
- [40] EUROSTAT, *Panorama of Transport*. Luxembourg: EU Off. Official Publications, 2009.
- [41] EPRI, "Environmental assessment of plug-in hybrid electric vehicles—Volume 1: Nationwide greenhouse gas emissions," vol. 1, Jul. 2007, Art. ID 1015325.
- [42] C. Camus, T. Farias, and J. Esteves, "Potential impacts assessment of plug-in electric vehicles on the Portuguese energy market," *Energy Pol.*, vol. 39, no. 10, pp. 5883–5897, 2011.
- [43] R. Marconato, *Electric Power Systems*, vol. 1, 2nd ed. Milan, Italy: CEI, 2002.
- [44] A. G. Hamilton, "Gaussian elimination," in *A First Course in linear Algebra*. Cambridge, U.K.: Cambridge Univ. Press, 1987, pp. 1–10. [Online]. Available: <http://dx.doi.org/10.1017/CBO9780511565731.002>